# Nonlinear Production of Suprathermal Tails in Auroral Electrons

D. L. Matthews, M. Pongratz,[1] and K. Papadopoulos[2]

*Institute for Fluid Dynamics and Applied Mathematics, University of Maryland, College Park, Maryland 20742*

Differential energy spectra of electrons observed in an auroral breakup show evidence that an incident electron beam of energy $E$ = 6–13 keV, width of 2–5 keV, and variable intensity was stabilized over a period of at least several minutes by the oscillating two-stream instability in the manner previously described by Papadopoulos and Coffey. The critical observed feature predicted by these authors' calculation is a tail with differential flux $dj/dE \propto E^{-0.5}$. This tail is much too intense to be attributed to the effects of collisions with atmospheric constituents. It is possible that the tail is part of the beam itself, i.e., produced higher up, but there are at least two arguments against this: first, the observations indicate that the tail approaches isotropy, whereas the beam is mostly downcoming, and second, the tail is observed as low as 130 km; the portion of the tail below 1.5 keV would have been absorbed by the atmosphere at greater heights if it had been incident from above. The observations support the hypothesis that the tail electrons are produced locally and by the proposed stabilization process. Implications are briefly discussed.

## 1. Introduction

The principal cause of discrete aurora is recognized to be precipitating electrons with energies in the range of about 100 eV to 100 keV. The processes that accelerate and precipitate these electrons are not well understood, but the manner in which they lose energy by collisions with atmospheric constituents has been quantitatively treated. Ionizing collisions by a kilovolt electron beam produce a steep strongly altitude-dependent tail of slowed-down secondary and backscattered electrons, which has been clearly described recently by *Banks et al.* [1974], *Berger et al.* [1974], and *Rees and Maeda* [1973]. Most of the electrons in this tail have energies of $\lesssim$30 eV.

In some cases, much more energetic tails have been observed in aurora, as is shown for example in Figure 1. The peaked region we call the beam, the tail being the part of the spectrum that rises toward lower energy. We assume, for reasons to be discussed later, that the tail is produced by interaction of the beam with the ionosphere. The above predictions of secondary flux in the energy range 0.5 to ~2 keV are at least a factor of 30 lower than these observations. Similar spectra have been observed by others [e.g., *Reasoner and Chappell*, 1973; *Arnoldy and Choy*, 1973].

In this paper we present new auroral electron energy spectra and hypothesize that a certain nonlinear local plasma interaction accounts for the observed tail. This hypothesis has been outlined earlier [*Papadopoulos and Coffey*, 1974*a*]. In addition to the tail, it predicts a spectrum of plasma turbulence and irregularities which will give rise to anomalous resistivity [*Papadopoulos and Coffey*, 1974*b*].

The present paper is organized as follows. In section 2 our rocket results are presented. In section 3 we describe the nonlinear beam stabilization process and how it produces a tail, and we show that the observed spectra are consistent with the theory and support our contention that the tail is produced locally. Section 4 discusses some implications.

## 2. Experimental Results

A Nike-Tomahawk sounding rocket was launched at Fort Churchill, Canada ($L \simeq 8$), on March 21, 1968, reaching an apogee of 240 km at 0606 UT. The breakup (expansive) phase of an auroral substorm began a few minutes earlier, at 0602 UT, just before launch. Active discrete auroral forms occurred over most of the sky during the flight with intensity IBC II, appropriate to the observed electron energy flux of ~10 ergs cm$^{-2}$ s$^{-1}$.

The instrument on board which obtained the data presented here was a spherical electrostatic analyzer with electron multiplier detectors. A full description of the instrument, its calibration, and the results may be found in the report by *Pongratz* [1972]. Briefly, the energy range between 0.5 and 40 keV was covered by 29 energy channels spaced in geometric progression, the energy resolution $\Delta E/E$ in each channel being constant at ~0.15. Count rates were high enough to ensure good statistics.

The spectra presented in this paper are averaged over one roll of the rocket and over two directions, downcoming (0° < $\alpha$ < 90°) and upgoing (90° < $\alpha$ < 135°), where $\alpha$ is the pitch angle. The upgoing data do not cover the entire range of pitch angles and so are somewhat less reliable than the downcoming data. One hundred and twenty-three spectra were produced.

The aurora was very active, and the rocket passed in and out of bright visible forms, but the observed electron spectra showed less variation than might have been expected. Figures 2–5 show two observed extremes plotted in various ways.

Since we intend to make a physical distinction between the beam and the tail, it is necessary to separate them in the data. We identify the fluxes from 0.5 to 1.4 keV as being entirely due to tail electrons. These points are well fitted by $\log f(V) = S \log V + \text{const}$ for each spectrum, i.e., the distribution function follows a power law. The fit was performed for each spectrum separately, and the resulting function was extrapolated and subtracted point by point from the rest of the spectrum, the differences being identified as the beam. The resulting parameters are summarized in Table 1. The tail number density $n_T$ was computed, somewhat arbitrarily, by extrapolation of the fitted tail function out to the beam peak speed $V_{max}$ and by integration. These procedures slightly overestimate the beam

[1] Now at Los Alamos Scientific Laboratory, Los Alamos, New Mexico 87544.

[2] Also at Naval Research Laboratory, Washington, D. C. 20375.

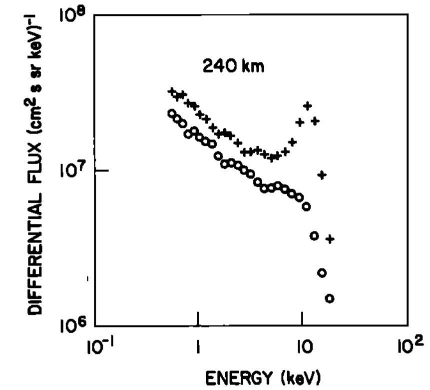


Fig. 1. Differential electron energy spectrum observed in a breakup aurora. Crosses represent downcoming flux and circles upgoing flux.

number density $n_B$. The 'Max' and 'Min' entries in the table are the maximum and minimum values of the various quantities observed during the whole flight excluding the last three spectra, which are summarized in the 'Last' entry. These three spectra were taken at altitudes below 135 km and show some degradation by atmospheric collisions, but the effect on the tail is less than would be expected in the absence of a local accelerating mechanism. This point is discussed further at the end of this section.

Owing to the moderate resolution (~15%) of the instrument with regard to energy and angle there is some overlap between the energy channels, resulting in some instrumental broadening of the narrowest peaks. The narrowest observed peak had a $\Delta V/V$ of 0.12, but as much as half of this width could be instrumental, hence the estimate of $(\Delta V/V)_{\min} \lesssim 0.1$ in the last column of Table 1. For $\Delta V/V \gtrsim 0.2$, instrumental broadening is negligible. In no case does it affect the beam intensities which are obtained by integration.

The following features are evident from Table 1:

1. The tail spectral index $S$ (i.e., slope on a log-log plot) is rather constant, lying between limits of $-0.9$ and $-1.25$. (To compare with the presentation of differential flux versus energy in the figures, divide values of $S$ by 2.)

2. The tail intensity $n_T$, the beam width $\Delta V/V_{\max}$ (where $\Delta V$ is the full width at $V = V_{\max}/2$), and the beam number density $n_B$ all vary over about a factor of 4 or 5 during the flight. The maximum differential number density $f(V_{\max})$ varies over a smaller range, about a factor of 3. The last three spectra show the effects of atmospheric attenuation at altitudes of 125–135 km and are listed separately in Table 1; one is plotted in Figure 6.

3. A least-squares fit of all 123 data points shows that $n_T = 2.3 n_B$ with a standard deviation of 15%. The data would admit a less simple relationship, such as a power law dependence, but the standard deviation would not be reduced. No time delay could be found between $n_B$ and $n_T$, but as the spectra are 2-s averages, delays less than 2 s would not be detectable.

4. On the other hand, we have estimated the net downward current measured by this instrument and cross-correlated it with the energy $E_{\max}$ at the beam peak. The most intense burst of the flight, which began at 4 min 30 s and lasted about 30 s, shows a clear 8-s delay between the major current bursts (from 4 to 8 × $10^8$ el/cm² s) and the corresponding peak energy jumps (from ~10 to 12 keV). The peak energy lags the current. In this region the beam is very broad, exemplifying its strong tendency throughout the flight to broaden at higher intensity. A similar lag of 4–5 s is noticeable in one later current peak (7 min 15 s to 7 min 28 s). In other parts of the flight that show this correlation between $E_{\max}$ and current, significant time delays are not found. These results indicate that at times a current-limited resistivity [*Ossakow*, 1968] may be playing a role in determining the beam energy but that it is not the only factor that affects the relationship between beam energy and current. The beam width $\Delta V/V$ shows little correlation with $n_B$ or $n_T$.

Electron density was measured with a retarding potential analyzer on the same flight and was found to vary only between 1 × $10^5$ and 2.5 × $10^5$ cm$^{-3}$. It was not correlated with any of the electron parameters discussed above. The same probe measured electron temperatures between 1000 and 2300 K, the maximum occurring during the major burst from 4 min 30 s to 5 min 0 s, indicating heating of the plasma electrons by the beam. No information is available on the ion or neutral temperature.

Before advancing a local plasma theory of tail formation we

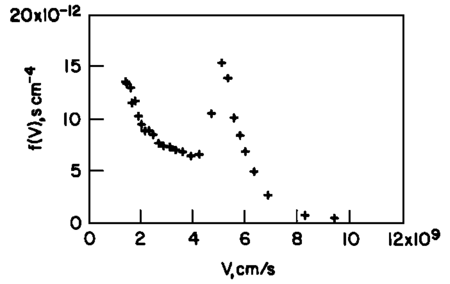


Fig. 2. One of the sharpest beams observed, plotted in the form of the one-dimensional velocity distribution function. All data in Figures 2–5 are downcoming fluxes.

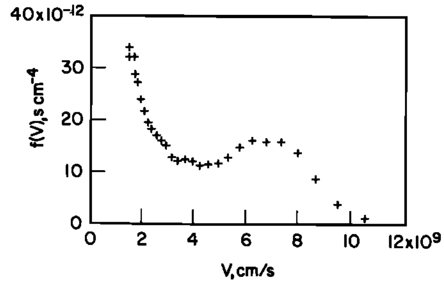


Fig. 3. One of the broadest beams observed, plotted as in Figure 2.

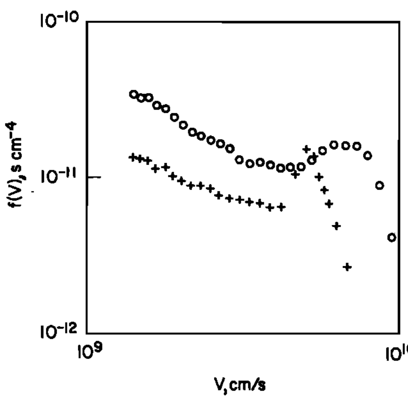


Fig. 4. Data of Figures 2 (crosses) and 3 (circles) on a logarithmic velocity scale.

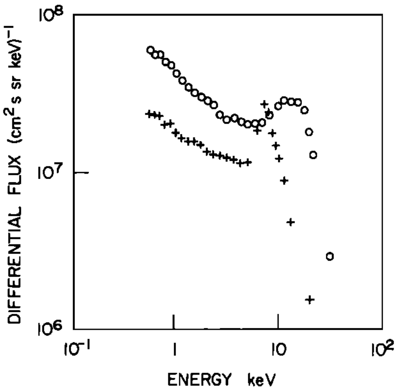


Fig. 5. Data of Figures 2 and 3 on a logarithmic flux-energy scale.

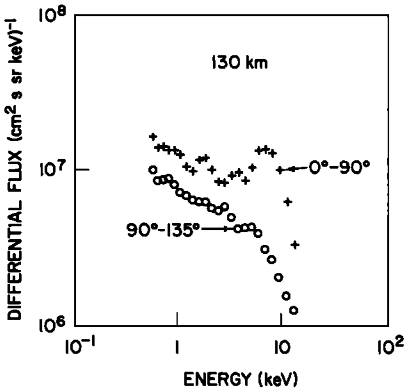


Fig. 6. Low-altitude spectrum. Crosses represent downcoming flux and circles upgoing flux. Compare with Figure 1.

need to show that the observed tail spectrum cannot be due to secondary electrons (plus degraded primaries) produced in inelastic collisions. The most complete and relevant calculations for our purpose have been performed by *Banks et al.* [1974]. They assumed an incident flux isotropic over the downward hemisphere with a Gaussian spectrum proportional to exp $[-(E - E_0)^2/2\sigma^2]$, with $E_0$ = 10 keV and $\sigma = 0.1E_0$, quite similar to one of our narrower observed beams. Figure 7 shows their calculated spectrum at 130 km with one of our observed spectra superimposed. Clearly, secondaries and degraded primaries are insignificant in the observed tail. The question remains whether it is produced locally or is part of the primary beam. In the latter case one would expect the tail to be cut off at altitudes low enough that the tail electrons are stopped but high enough that the more energetic electrons in the beam are able to penetrate with only moderate degradation. Banks et al. have also calculated this effect by starting above the atmosphere with a spectrum observed by *Reasoner and Chappell* [1973] which is rather similar to ours. We have interpolated and appropriately normalized Figure 13 of Banks et al. to obtain the spectrum expected at 132 km and have superimposed our own spectrum taken at ~130 km, the same as that shown in Figures 6 and 7. The comparison is seen in Figure 8. Note that our observed spectrum is rising toward low energy in the 0.5-keV region, whereas the calculated spectrum is falling. Some process is regenerating the tail, and it is reasonable to suppose that the same mechanism is acting throughout the flight, because the 130-km spectrum has very much the same shape as all the others, although it is somewhat reduced in intensity. The mechanism must, however, be able to compete with the high electron-neutral collision frequency of $2 \times 10^3$ at 130 km. We will return to this question after presenting the theory.

## 3. THEORETICAL MODEL

It has been shown in previous papers [*Papadopoulos and Coffey*, 1974*a*, *b*] that several of the observations of precipitating auroral particles and the fact that they propagate essentially uninhibited to low altitudes, where they are collisionally absorbed, are consistent with the concepts of nonlinear stabilization of beam-plasma instabilities by parametric effects [*Papadopoulos et al.*, 1974; K. Papadopoulos, unpublished manuscript, 1975]. The basis of this mechanism is fast transfer of plasma waves from regions in $k$ space in resonance with the beam to regions in resonance with the ionospheric electrons, where they can be absorbed very efficiently by the plasma and create upstreaming and downstreaming electron fluxes (tails) in the energy region intermediate between the energy of the precipitating electrons and the ambient electron temperature.

The details of the nonlinear stabilization process have already been described in the above publications and will not be repeated here. The overall physical picture is shown in Figure 9. The fast precipitating electrons create plasma waves in region I. When these waves exceed a threshold level, a fast energy transfer occurs toward regions of smaller phase velocity (larger wave number) labeled as II in Figure 9, and ion density fluctuations $W_s$ are produced. These secondary waves $W_2$ can interact efficiently with the shaded part of the distribution function and thus create tails (dashed lines). These processes occur only if the precipitating electrons are not prevented by collisions from creating the primary spectrum of plasma waves. As we will see, this was the case for all the experimental cases that we will discuss.

Our overall picture can be presented as the interplay of three separate processes which we identify as (1) creation of the primary wave spectrum I ($W_1$), (2) energy transfer from the primary spectrum $W_1$ to the secondary spectrum $W_2$ (regions II) and $W_s$, and (3) local particle acceleration and tail creation. We discuss below each of these components separately.

*Primary wave spectrum.* It is well known [*Krall and Trivelpiece*, 1973] that when a tenuous stream of electrons with an average directed velocity $V_0 > 3V_e$, where $V_e$ is the thermal velocity of the plasma, and with a spread in velocities $\Delta V < V_0$ passes through the auroral plasma, a beam-plasma instability occurs, leading to the excitation of longitudinal plasma waves with wave numbers around $k_0 \approx \omega_e/V_0$ in an interval $\Delta k/k_0 \approx \Delta V/V_0$ and with a growth rate

TABLE 1. Range of Observed Spectral Parameters

| | $n_B$, cm$^{-3}$ | $n_T$, cm$^{-3}$ | $S$ | $V_{max}$, $10^{10}$ cm/s | $E_{max}$, keV | $f(v_{max})$, $10^{-10}$ cm$^{-4}$ s | $\Delta V/V$ |
|---|---|---|---|---|---|---|---|
| Max | 0.3 | 0.8 | −1.25 | 0.73 | 13 | 0.24 | 0.5 |
| Min | 0.07 | 0.2 | −0.9 | 0.5 | 7 | 0.07 | ≲0.1 |
| Last | 0.07 | 0.15 | −0.75 | 0.48 | 6.5 | 0.05 | 0.3 |

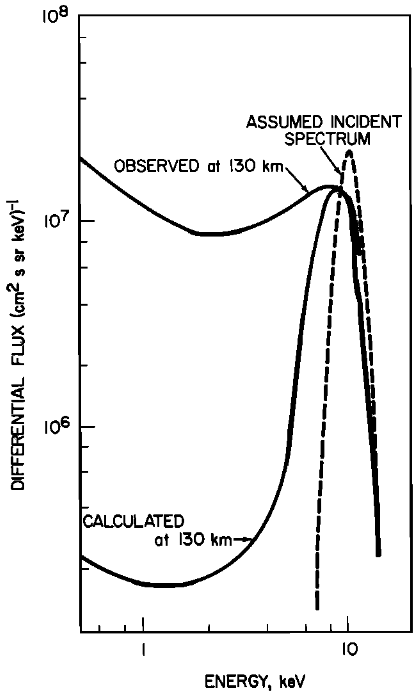


Fig. 7. Calculated effect of atmospheric scattering on a sharp incident beam (dashed line), compared with observed spectrum (smoothed from Figure 6).

$$\gamma \approx \frac{\pi}{2} \frac{n_B}{n} \left( \frac{V_0}{\Delta V} \right)^2 \omega_e \quad (1)$$

where $n_B$ and $n$ are the densities of the beam and the auroral plasma, respectively, and $\omega_e$ is the plasma frequency. The excited waves are directed predominantly in the beam direction. This process will occur only in regions where the collisional

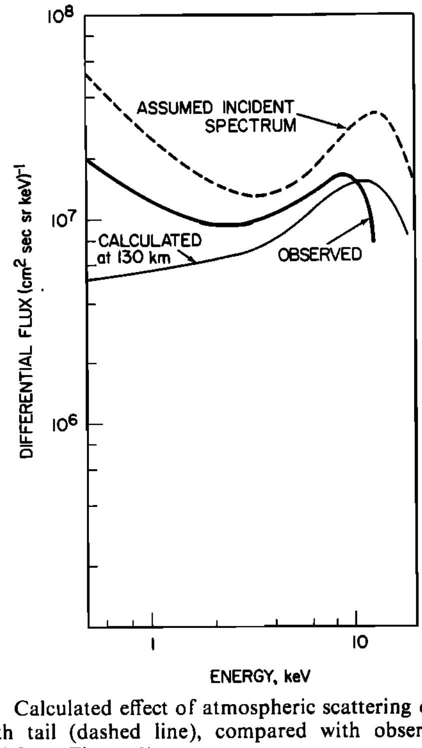


Fig. 8. Calculated effect of atmospheric scattering on an incident beam with tail (dashed line), compared with observed spectrum (smoothed from Figure 6).

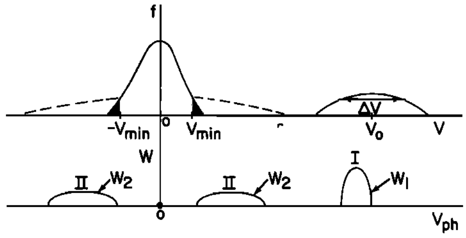


Fig. 9. Schematic of nonlinearly stabilized beam in one dimension. Particle velocities in the thermal plasma and the beam are indicated with solid lines and in the tail with dashed lines. Phase velocities of the associated waves are shown in the lower part of the diagram. The small shaded parts of the thermal distribution are those affected by the secondary waves (regions II).

damping rate due to electron-ion and electron-neutral collisions is smaller than the generation rate $\gamma$. This leads to the conditions

$$2 \frac{\pi}{2} \frac{n_B}{n} \left( \frac{V_0}{\Delta V} \right)^2 > \frac{1}{n \lambda_D^3} \quad (2a)$$

$$2 \frac{\pi}{2} \frac{n_B}{n} \left( \frac{V_0}{\Delta V} \right)^2 > \frac{\nu_{en}}{\omega_e} \quad (2b)$$

where $\nu_{en}$ is the electron-neutral collision rate. Restriction (2) is a basic requirement for the validity of the theory as presented below.

If we neglect nonlinear processes, the evolution of the system is described by the well-known quasi-linear theory. The details of this theory are by now a textbook matter [*Davidson*, 1972; *Krall and Trivelpiece*, 1973]. According to this theory, since the plasma wave generation is due to the beam with negative slope ($(\partial f / \partial V) < 0$), these particles lose their energy rapidly, and the inside slope of the stream begins to move into the region of low velocities. As a result, the distribution function of the stream changes from bell-shaped to table-shaped, increasing in width to one side and correspondingly losing height as the total number of particles in the beam is conserved. In this fashion the electron stream quickly relaxes to a plateau with $(\Delta V / V_0) \sim 1$, and at that time the energy of the plasma waves is given by

$$W_1^Q = \tfrac{1}{6} n_B m V_0^2 \quad (3)$$

The symbol $W_1^Q$ indicates the wave energy at quasi-linear stabilization. This result is based on the theory of an infinite homogeneous plasma completely penetrated by the beam. However, our situation is substantially different, since there are two definite boundaries. The first boundary corresponds to the region where the beam is initially formed or injected and the second to where it is absorbed. The generalization of the quasi-linear theory for the beam injection in a finite region can be found in the work by *Tsytovich* [1970] and results in an increase of the maximum wave energy over the one given by (3). Physically, this is due to the fact that the waves generated by the stream move with very slow velocity with respect to the fast electrons, since $V_{gr} = 3(V_e/V_0)V_e \ll V_0$. This implies that the fast electrons as they move with velocity $V_0$ from one point in space to another are acted upon not only by the waves they themselves generate but by waves generated earlier by other particles. This creates an oscillation pileup effect, which results in a substantial increase in the level of the maximum wave energy density $W_1$ over that to be expected from simple quasi-linear theory. The results as given in the work by *Tsytovich* [1970, chap. 6] are that the maximum energy density $W_1^m$ is

$$W_1^m = W_1^Q \frac{V_0}{V_{gr}} \tag{4}$$

where the group velocity $V_{gr}$ of the waves is

$$V_{gr} = 3 \frac{V_e}{V_0} V_e \tag{5}$$

This is correct only if the pileup distance $x_0 = V_{gr}/\gamma$ is smaller than the inhomogeneity length. Since typically $x_0$ is of the order of 10–200 m, this condition is easily satisfied for the case under consideration.

*Nonlinear energy transfer.* We examine next the following problem. Given a plasma wave spectrum $W_1$ in the wave number region $k_0$, what is the threshold value for parametrically creating lower phase velocity waves ($k > k_0$) which can interact with the plasma and thus create the fast tails? The mathematical details can be found in the article by K. Papadopoulos (unpublished manuscript, 1975). It is found that the threshold for the instability is given by [*Papadopoulos et al.*, 1974]

$$\frac{W_1^T}{nT_e} = (k_0\lambda_D)^2 \frac{\Delta k}{k_0} \tag{6}$$

and the maximum wave number of the secondary waves is given by [*Abdulloev et al.*, 1974]

$$k_m\lambda_D \sim \left(\frac{W_1}{nT}\right)^{1/2} \tag{7}$$

(One should notice that besides the above instability, which is known as oscillating two-stream instability (OTS) in the U.S. literature or quasi-decay in the Soviet literature, there is another instability with $k < k_0$ called modulation instability [*Vedenov and Rudakov*, 1964].) Results (6) and (7) can be seen from the following qualitative considerations. The nonlinear dispersion relation [*Tsytovich*, 1970] for plasma waves in the presence of $W_1$ is given by

$$\omega = \omega_e + \frac{3}{2}\frac{k_0^2\lambda_D^2}{\omega_e} - \alpha\omega_e \frac{W_1}{nT} \tag{8}$$

where $\alpha$ depends on the spectral shape but is of the order of unity. When the third term of (8) exceeds the second term, there is an energetic collapse of the plasma waves from $k_0$ to $k \approx k_m$, because the attractive potential energy $\alpha(W_1/nT)\omega_e$ exceeds the kinetic energy $\frac{3}{2}k_0^2\lambda_D^2/\omega_e$. (Ion waves may also be produced, but the fraction of energy going into these waves must be less than $(m_e/m_i)^{1/2}$ (Manley-Rowe relation) relative to the electron plasma oscillations, i.e., less than 1/170 for $O^+$ ions, so the ion waves can be neglected.)

*Local acceleration due to turbulence.* From the previous discussion we can see that the precipitating electrons create a primary spectrum of plasma waves $W_1$ which subsequently decays to a secondary spectrum $W_2$ of lower phase velocity. We attribute to $W_2$ the local acceleration mechanism which creates the fast electron tails of the auroral electron distribution function. The energy of the plasma waves $W_2$ is absorbed by the fast particles with speed $V > \omega_e/k_m$, and thus their energy is further increased. A plasma wave with phase velocity $V_p$ can be absorbed in a nonbremsstrahlung mechanism by a particle only if the velocity of the particle is larger than $V_p$, so that a small number of particles which already have high energies are accelerated. When their velocities increase, such particles can absorb a larger number of plasma waves and thus further increase their energy. A detailed description of the acceleration including the dynamic behavior of $W_2$ constitutes a formidable problem of plasma turbulence still awaiting solution. We try to solve here a simplified problem in the hope of finding some quantitative estimates and some qualitative properties of the acceleration mechanism. We consider the evolution of a distribution $f_T$ of suprathermal electrons in the presence of a one-dimensional steady spectrum of turbulence $W_2(k)$, with $W_2 = \int dk\, W_2(k)$, in resonance with the particles. The time evolution of the distribution function is given by

$$\frac{\partial f_T}{\partial t} = \frac{\partial}{\partial V} D \frac{\partial}{\partial V} f_T + C(\nu_{en}, f_T) \tag{9}$$

where $C(\upsilon_{en}, f_T)$ is an appropriate collisional term describing the relaxation of the tails due to the collisions of the fast electrons with the neutrals, and the diffusion coefficient $D(V)$ along the magnetic field is given by

$$D(V) = \frac{\pi\omega_e^2}{mnV} W_2\left(k = \frac{\omega_e}{V}\right) \tag{10}$$

We discuss now a simple model that can provide a description of the characteristics of the tail. We assume first a simple collision integral $C = \upsilon_{en} f_T$, where $\upsilon_{en}$ is the proper function of velocity, which for electron-neutral collisions above 1 keV is of the form $\nu_{en} \propto 1/V$. In order to determine the velocity dependence of the diffusion coefficient we need the velocity dependence of $W_2$ ($k = \omega_e/V$). Since the energy transfer rate for the waves $W_2$ is essentially the same for all the neighboring wave numbers, the spectral form will be determined by wave damping. In the paper by *Papadopoulos and Coffey* [1974*a*] the calculation was performed for a collisionless plasma, so the wave damping was essentially the Landau damping of the tails. In the present case the dominant damping mechanism is electron-neutral collisions. Following *Papadopoulos and Coffey* [1974*a*] we find that $W_2(V) \propto [1/\nu_{en}(V)] \propto V$ and $D(V) \propto$ const. An estimate of the average energy of a tail electron $\bar{\epsilon}_T$ is given by

$$\bar{\epsilon}_T \approx m\bar{D}\cdot\bar{t}_{en} \tag{11}$$

where $\bar{D}$ is the average value of the diffusion coefficient and $\bar{t}_{en}$ the average electron-neutral collision time in the appropriate energy range. From (10) and (11) we find

$$\frac{\bar{\epsilon}_T}{T_e} \approx 2(k_2\lambda_D)^{-1}\frac{\omega_e}{\bar{\nu}_{en}}\frac{W_2}{nT_e} \tag{12}$$

The velocity spectrum of the tails can be found by balancing the acceleration rate $\gamma_a \propto D/V^2$ with the collision rate $\nu_{en} \propto 1/V$, which for $D \propto$ const gives $f_T \propto 1/V$, consistent with the observations.

The local acceleration mechanism described previously affects only particles whose velocity is at least as large as the lowest value of the velocity for which $W_2(V) \neq 0$, which we define as $V_{min}$ (Figure 9). The particle density in the tails $n_T$ will then be given by

$$n_T = \int_{V_{min}}^{V_0} dV f(V) \tag{13}$$

where $f(V)$ is the distribution function of the ambient plasma without any consideration of plasma processes. This is composed of a cold Maxwellian with temperature of the order of 0.1 eV and a power law tail due to the production of secondaries which extends to 200–300 eV for the altitudes of interest [*Banks et al.*, 1974; *Rees and Maeda*, 1973]. The energy $W_1^{st}$

required to stabilize the electron stream nonlinearly can be found by equating the nonlinear transfer rate $\gamma_{NL}(W_1)$ from region I to regions II to the wave growth of $W_1$ as given by (1). Since [*Papadopoulos et al.*, 1974; K. Papadopoulos, unpublished manuscript, 1975]

$$\gamma_{NL}(W_1) \approx \omega_e\left(\frac{m}{M}\right)^{1/2}\left(\frac{W_1}{nT}\right)^{1/2}$$

where $M$ is the ion mass, we find

$$\frac{W_1^{st}}{nT} \approx 50\left(\frac{n_B}{n}\right)^2\left(\frac{V_0}{\Delta V}\right)^4\left(\frac{M}{m}\right) \qquad (14)$$

The value of the wave number $k_m$ is given by [*Abdulloev et al.*, 1974]

$$k_m\lambda_0 \approx \left(\frac{W_1}{nT}\right)^{1/2} \qquad (15)$$

If we assume a $1/V^n$ dependence of the resulting tail, we find from (13)–(15)

$$n_T \propto k_{\min}^{n-1}$$

with $n$ to be determined from the distribution of the secondaries.

*Overall description and scalings.* On the basis of the above we have the following scheme of energy transfer (Figure 9). The precipitating electrons excite plasma waves in region I. These subsequently decay to lower phase velocity waves, which interact with the ambient particles producing the tails.

On the basis of (1)–(9) we examine below whether the data described in the previous section are consistent with the theoretical limitations of the model and the implied scaling laws. For purposes of numerical comparison we consider the following values as typical: $n_B = 0.3$ cm$^{-3}$, $V_0/\Delta V \approx 5$, $V_0/V_e \approx 200$, $n \approx 10^5$ cm$^{-3}$, $\omega_e = 2 \times 10^7$ s$^{-1}$, and $\lambda_D \approx 1$ cm.

We examine first whether the conditions given by (2) are satisfied. Equation (2*a*) implies that

$$n_B\left(\frac{V_0}{\Delta V}\right)^2 > \tfrac{1}{3}\lambda_D^{-3}$$

which is easily satisfied for the typical conditions.

Equation (2*b*) implies that our theory is correct down to altitudes such that $\nu_{en}/\omega_e < \pi(n_B/n)(V_0/\Delta V)^2$. For the typical values this corresponds to $\nu_{en} < 5000$. Since the lowest altitude under study is 130 km, where $\nu_{en} \approx 2000$ s$^{-1}$, we have no problem satisfying (2*b*) over the range of interest.

In order to produce the secondary wave spectrum $W_1^{\max} > W_1^T$, we have from (4), (5), and (6) that

$$\frac{1}{18}\left(\frac{n_B}{n}\right)\left(\frac{V_0}{V_e}\right)^4 > \frac{9}{4}\left(\frac{V_e}{V_0}\right)^2\frac{\Delta V}{V_0}$$

or

$$\left(\frac{n_B}{n}\right) > 36\left(\frac{V_e}{V_0}\right)^6\frac{\Delta V}{V_0} = 36\left(\frac{T_e}{\epsilon_B}\right)^3\frac{\Delta V}{V_0}$$

which is also easily satisfied for the typical values.

To compute the energy of the tails we consider (12), with $W_2 \approx W_1^{st}$ and $k_1 \approx k_m$ as given by (14) and (15) and $\bar{\nu}_{en} \approx 10^3$; we find thus that $\bar{\epsilon}_T/T_e \approx 3 \times 10^3$ or $\bar{\epsilon}_T \approx 1$ keV, which agrees with the average energy observed. Finally, since $n_T \propto k_{\max}^{n-1}$ and from (14) and (15) $k_{\max} \propto n_B$, the observed $n_T \propto n_B$ dependence seems to imply that the initial low-energy nonthermal secondary tail distribution is a power law with $n = 2$ (i.e., $1/V^2$ dependence).

## 4. DISCUSSION

The experimental results presented here indicate that the collisionless plasma processes discussed in the paper by *Papadopoulos and Coffey* [1974*a*] are important in understanding the nonthermal features of the auroral plasma even at low altitudes. It appears that for electrons of energy $\gtrsim 30$ eV the nonlinear plasma process competes with or completely dominates the effects of collisions. Observation and theory agree that such energetic tails may be formed not only at heights great enough that collisions are unimportant but also in the $E$ region, where not only are collision frequencies high for thermal electrons but also the density is so great that tail electrons formed at greater heights could not penetrate.

Thorough studies of existing auroral electron data, together with new, comprehensive in situ observations of particles, waves, and plasma parameters including conductivity, are being planned in order to establish the range of parameters over which the nonlinear process operates. Observation of ionization irregularities, or measurement of enhanced resistivity, will be crucial. At present we can say that our spectra and those observed by *Arnoldy and Choy* [1973] and *Reasoner and Chappell* [1973] are consistent with the theory. We have not yet found any counterexamples. The range of parameters in these three sets of measurements is roughly as follows: $\nu_{en}$, up to 2000 s$^{-1}$; $n$, $10^4$ to $3 \times 10^5$ cm$^{-3}$; beam energy at peak, 1–12 keV; beam energy flux, 0.1–10 ergs cm$^{-2}$ s$^{-1}$; and net current, up to $3 \times 10^{-10}$ A/cm$^2$, usually but not always corresponding to a net downward flux of electrons.

It has been noted in the paper by *Papadopoulos and Coffey* [1974*b*] that such plasma processes can be responsible for the creation of anomalous resistivity in the ionosphere and magnetosphere, from altitudes of 130 km to perhaps several thousand kilometers. Such resistivity could reach more than $10^4$ times the Spitzer value and could support a substantial electric field parallel to the earth's magnetic field without producing runaway or excessive heating of the thermal plasma. Such an electric field, if it is first established by some other process, could further accelerate some electrons, leading to positive feedback.

If an auroral beam consists of electrons accelerated through an electrostatic potential, the same potential can also reflect backscattered electrons and increase the intensity of the downcoming secondary component, as discussed by *Evans* [1974]. It does not appear that the model used by Evans can generate a tail as energetic and intense as we report here, and it certainly could not regenerate the tail locally in competition with collisions in the $E$ region as our data appear to require. Nevertheless, this factor would have to be included in a full calculation.

Finally it should be noted that the theory outlined here is one-dimensional. Extension to two and three dimensions is under way. We expect the same qualitative conclusions from the more complete theory.

*Acknowledgments.* S. McPhillips and K. Christoph, with essential contributions from E. Grossenbacher and his machine shop staff, were responsible for the sound design and construction of the payload. Launch support was provided by the Churchill Research Range, operated at that time by the U.S. Air Force. Many members of the staff of the NASA Goddard Space Flight Center provided integration and launch support. This work was supported by NASA under research contract NSR 21-022-077 and by the Computer Science Center of the University of Maryland.

The Editor thanks D. W. Swift and another referee for their assistance in evaluating this paper.

## REFERENCES

Abdulloev, Kh. O., I. L. Bogljubskii, and V. G. Makhankov, Dynamics of Langmuir turbulence, *Phys. Lett., Sect. A, 48,* 161, 1974.

Arnoldy, R. L., and L. W. Choy, Auroral electrons of energy less than 1 keV observed at rocket altitudes, *J. Geophys. Res., 78,* 2187–2200, 1973.

Banks, P. M., C. R. Chappell, and A. F. Nagy, A new model for the interaction of auroral electrons with the atmosphere: Spectral degradation, backscatter, optical emission, and ionization, *J. Geophys. Res., 79,* 1459–1470, 1974.

Berger, M. J., S. M. Seltzer, and K. Maeda, Some new results on electron transport in the atmosphere, *J. Atmos. Terr. Phys., 36,* 591–618, 1974.

Davidson, R. C., *Methods in Nonlinear Plasma Theory,* chap. 9, Academic, New York, 1972.

Evans, D. S., Precipitating electron fluxes formed by a magnetic field aligned potential difference, *J. Geophys. Res., 79,* 2853–2858, 1974.

Krall, N. A., and A. W. Trivelpiece, *Principles of Plasma Physics,* chap. 9, McGraw-Hill, New York, 1973.

Ossakow, S. L., Anomalous resistivity along lines of force in the magnetosphere, *J. Geophys. Res., 73,* 6366–6369, 1968.

Papadopoulos, K., and T. Coffey, Nonthermal features of the auroral plasma due to precipitating electrons, *J. Geophys. Res., 79,* 674–677, 1974*a*.

Papadopoulos, K., and T. Coffey, Anomalous resistivity in the auroral plasma, *J. Geophys. Res., 79,* 1558–1561, 1974*b*.

Papadopoulos, K., M. Goldstein, and R. Smith, Stabilization of electron streams in type III solar bursts, *Astrophys. J., 190,* 175–185, 1974.

Pongratz, M. B., Observations of interchange between acceleration and thermalization processes in auroral electrons, *Tech. Note BN-737,* Inst. for Fluid Dyn. and Appl. Math., Univ. of Md., College Park, June 1972.

Reasoner, D. L., and C. R. Chappell, Twin payload observations of incident and backscattered auroral electrons, *J. Geophys. Res., 78,* 2176–2186, 1973.

Rees, M. H., and K. Maeda, Auroral electron spectra, *J. Geophys. Res., 78,* 8391–8394, 1973.

Tsytovich, V. N., *Non-Linear Effects in Plasma,* chap. 6, Plenum, New York, 1970.

Vedenov, A. A., and L. I. Rudakov, Wave interactions in continuous media, *Dokl. Akad. Nauk SSSR, 159,* 767, 1964.

(Received April 11, 1975;
accepted July 10, 1975.)